

# Efficient Quantum Information Transfer Through a Uniform Channel

Regular Paper

Leonardo Banchi<sup>1,2</sup>, Tony J. G. Apollaro<sup>1</sup>, Alessandro Cuccoli<sup>1,2</sup>,  
Ruggero Vaia<sup>3</sup> and Paola Verrucchi<sup>3,1,2\*</sup><sup>1</sup> Dipartimento di Fisica e Astronomia, Universita' di Firenze, Italy<sup>2</sup> Istituto Nazionale di Fisica Nucleare, Sezione di Firenze, Italy<sup>3</sup> Istituto dei Sistemi Complessi - CNR, Italy\*Corresponding author E-mail: [verrucchi@fi.infn.it](mailto:verrucchi@fi.infn.it)

Received 9 May 2011; Accepted 18 June 2011

**Abstract** Effective quantum-state and entanglement transfer can be obtained by inducing a coherent dynamics in quantum wires with homogeneous intrawire interactions. This goal is accomplished by optimally tuning the coupling between the wire endpoints and the two qubits there attached. A general procedure to determine such value is devised, and scaling laws between the optimal coupling and the length of the wire are found. The procedure is implemented in the case of a wire consisting of a spin-1/2 XY chain: results for the time dependence of the quantities which characterize quantum-state and entanglement transfer are found of extremely good quality also for very long wires. The present approach does not require engineered intrawire interactions nor a specific initial pulse shaping, and can be applied to a vast class of quantum channels.

**Keywords** spin chains, dynamics, quantum channels, entanglement

## 1. Introduction

Quantum communication and computation protocols are commonly based on the possibility of producing a pair of distant qubits which are in an entangled state. In the case

of solid state devices, which are suitable components of a quantum computer, the requirement is to transfer quantum information between localized qubits over relatively short distances within the device [1].

In this paper we consider qubits encoded in  $S=1/2$  spins, and the distant qubits between which the state transmission must be realized interact through a channel (or wire) consisting of a spin-1/2 chain, although the quantum-transport strategy we are going to depict can be generalized to different systems, as, e.g., Josephson arrays [2], quantum dot chains [3,4], or electrons diffusing in one dimension [5].

The general scheme we propose is illustrated in Fig.1: the aim is to efficiently transfer from the qubit A (Alice) to the distant qubit B (Bob) the property of being entangled with an external 'ancilla' qubit A'. To this goal we exploit the dynamics of the channel, for which we make only very basic and realistic assumptions about the internal couplings and the endpoint ones to A and B. Indeed, although several realizations of a channel have been proposed [6, 7], many are often subject to important adjustments of the intrawire interactions that are difficult (if not impossible) to realize experimentally [8, 9], while others require Alice and Bob to hold control of several neighboring qubits within the wire [10,11].

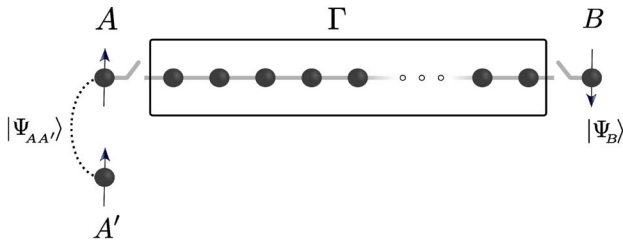


**Figure 1.** The endpoints of a quantum channel  $\Gamma$  are coupled to the qubits A and B, via a switchable interaction  $j$ ; A can be entangled with an external qubit  $A'$ .

We are going to show that coherent propagation can also be obtained by means of experimentally realistic setups, where (i) the wire is completely uniform and the only end-point couplings may be different, (ii) the transmission velocity coincides with the group velocity of the relevant excitations (yielding minimal transmission times), and (iii) very long wires can be used as the quality of the quantum-state and entanglement transfer is not substantially affected by the wire length.

## 2. Ballistic transmission through a uniform channel

As stated above, the channel (Fig.1) is realized by a uniform (i.e., with identical exchange coupling  $J=1$  between neighbors) spin chain  $\Gamma$  of length  $N$ , to which an external magnetic field  $h$  can be applied. In particular, in this paper we choose the XY model, which also allows for an anisotropy parameter  $\gamma$  and can be analytically approached through a transformation into an interacting fermion system [12]. We do also consider the isotropic XY model, defined by a vanishing anisotropy parameter  $\gamma$ , and usually referred to as the XX model.

The only interactions that can be different are the endpoint exchange coupling  $j$  to A and B, and the local magnetic field  $h_0$  on A and B; these parameters are assumed to be identical for A and B, so that the overall system is mirror-symmetric.

Using the labels  $i=1, \dots, N$  for the chain and  $i=0$  and  $i=N+1$  for the endpoint spins A and B, the total Hamiltonian reads

$$H = -\sum_{i=1}^{N-1} \left[ (1+\gamma) S_i^x S_{i+1}^x + (1-\gamma) S_i^y S_{i+1}^y \right] - h \sum_{i=1}^N S_i^z + j \sum_{i=0,N} \left[ (1+\gamma) S_i^x S_{i+1}^x + (1-\gamma) S_i^y S_{i+1}^y \right] - h_0 (S_0^z + S_{N+1}^z). \quad (1)$$

Furthermore, we also require the quantum-state transfer between A and B to occur in the shortest possible time, at variance with those approaches where perfect transmission is obtained in the regime of very tiny endpoint coupling, at the expense of waiting orders of magnitude larger times than the typical one for ballistic

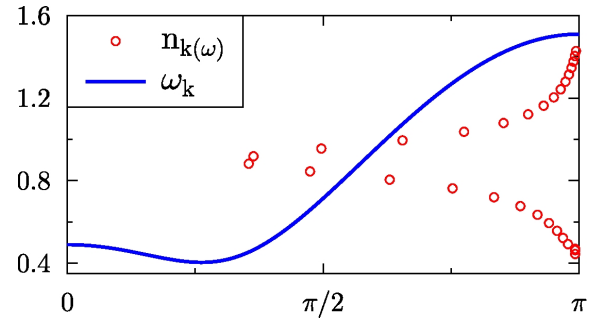


**Figure 2.** Dispersion relation of the spin-1/2 XY chain for  $\gamma = 0.5$  and  $h = 0.54$ . The bell-shaped distribution  $n_{\text{opt}}(\omega)$  (circles) is the optimized density of excitations vs.  $\omega$ , corresponding to  $h_0=0.85$  and  $j=0.48$

transmission [13, 14]. The first observation is that a crucial role is played by the dispersion relation  $\omega_k$  of the elementary excitations of the wire: if it were linear,  $\omega_k = \text{const} + vk$ , any perturbation would travel from A through the wire without changing its shape and a snapshot after the ballistic transmission time  $t_N = N/v$

should show the same perturbation sitting at B, as mirror symmetry suggests. However, our purpose to work with a uniform wire prevent us from dealing with a linear dispersion relation: a representative case is reported in Fig.2. Nevertheless, one can observe that almost coherent wavepacket propagation can still occur provided that the  $k$ -space components of the packet lie in a region where the dispersion relation is almost linear, namely around an inflection point  $k_0$  [15], where  $\omega_k \sim v(k-k_0)$ , being  $v = \partial\omega/\partial k|_{k_0}$  the group velocity at  $k_0$ . This fact was exploited to yield efficient transmission over a ring in Ref.[10]: there, in order to properly shape the excitation wavepacket, the authors proposed that both Alice and Bob had to initialize and decode a sizeable number of their neighbors. At variance with this, in Ref. [16] it has been shown that, initially taking the channel in its ground state  $|\Omega\rangle$  (though, other choices are possible), the dynamics following the initialization of the endpoint qubit A effectively creates a propagating wavepacket whose distribution in  $k$ -space,  $n(k)$ , can be controlled by modifying the endpoint interactions: if these are chosen such that  $n(k)$  is peaked around the flex  $k_0$  then a coherent propagation is expected. It is obvious that also the characteristic width  $\Delta$  of  $n(k)$  plays a relevant role: to get a real-space packet of small width  $\sigma$  (which must satisfy the relation  $2\sigma\Delta \geq 1$ ) one needs a large  $\Delta$ , but if it is too large then  $n(k)$  includes modes from the nonlinear part of  $\omega_k$  that would cause dispersive decoherence of the packet. As shown in Ref. [16], a trade-off between these regimes leads to an optimal value of  $\Delta$ , which can be tuned by means of the endpoint interactions  $j$  and  $h_0$ . It appears that varying  $h_0$  mainly affects the peak position of  $n(k)$ , while  $\Delta$  is predominantly affected by  $j$ . This can be explained considering that a larger  $h_0$  produces an initial overall state with larger energy, so  $n(k)$  must

include larger frequencies, while decreasing  $j$  will increase the time scale of the initial dynamics resulting in a broader real-space pulse, i.e., with smaller  $\Delta$ . Reasoning in terms of Gaussian-like wavepackets, the optimal value of  $\Delta$  results then [16]

$$\Delta_{opt} \approx \left( \frac{3|a|N}{2v} \right)^{-1/3} \quad (2)$$

where  $a$  is the coefficient of the cubic term in the expansion of  $\omega_k$  around the flex  $k_0$ .

### 3. Optimal transfer in the XY chain

As a first application of the optimization procedure we consider the isotropic ( $\gamma=0$ ) version of the XY model (the so called XX model) with no external magnetic field,  $h=0$ . In this case,  $\omega_k=\cos(k)$  and several analytical expressions are available [13]. The inflection point  $k_0=\pi/2$  corresponds to  $\omega_{k_0}=0$  and we hence set  $h_0=0$ . The width of  $n(k)$  only depends on the coupling  $j$  and reads  $\Delta= j^2/(2-j^2)$ . Therefore, Eq.(2) ensures the existence of an optimal coupling  $j_{opt}$  which, at leading order, is

$$j_{opt} \propto N^{-1/6} \quad (3)$$

In the XY case the analytical expressions are more complicated and the optimal parameters are found numerically.

Let us now give a panoramic view upon the resulting dynamics of the overall system. Fig.3 shows the time evolution of the magnetization parallel to the quantization axis all along the wire,  $\langle S_i^z(t) \rangle$ ,  $i=0,1, \dots, N, N+1$ , where  $N=50$  and initially the qubits A, B are in the states  $|\uparrow\rangle$  and  $|\downarrow\rangle$ , respectively. The difference between the upper panel, where all interactions are homogeneous ( $j=1$ ), and the lower panel, where  $j$  is given by Eq.(3), is striking: in the latter the induced coherent propagation makes  $\langle S_B^z(t^*) \rangle$  at the arrival time  $t^* \sim N$ , an almost perfect reproduction of the initial magnetization  $\langle S_A^z(0) \rangle$  of the qubit A, while in the upper panel the dynamics is apparently more dispersive.

As pointed out in [16] this peculiar dynamics induces also a high-quality quantum-state transmission. Here we consider the transmission of entanglement, following the scheme of Fig.1: the state of qubit A, which at  $t=0$  is maximally entangled with  $A'$ , propagates through the wire when  $j$  is switched on; if the information were transmitted exactly, at some arrival time  $t^*$  the qubit B should be maximally entangled with  $A'$ . Therefore, the natural estimator of the quality of entanglement transmission is the maximum (reached at  $t^*$ ) of the concurrence between  $A'$  and B in its time evolution,

$C(t) \equiv C(\rho_{BA'}(t))$  [17]. The state  $\rho_{BA'}(t)$  essentially depends on the dynamical non-equilibrium correlation functions between the components of qubits B and  $A'$ , and can be analytically approached through the mapping into an interacting fermion system, along with quantum information theoretic techniques [16]. Fig.4 shows the dynamics of the concurrence in the case of an XX chain, where  $N=50$ , as a function of time  $t$  and coupling  $j$ . For non-perturbative fixed coupling  $j$ ,  $C(t)$  reaches its maximum value at  $t^* \sim N$  as it can be analytically proven. Remarkably,  $C(t^*)$  takes its maximum when  $j=j_{opt} \sim 0.58$ , i.e., the optimal value predicted by Eq.(3), confirming that such prescription is correct.

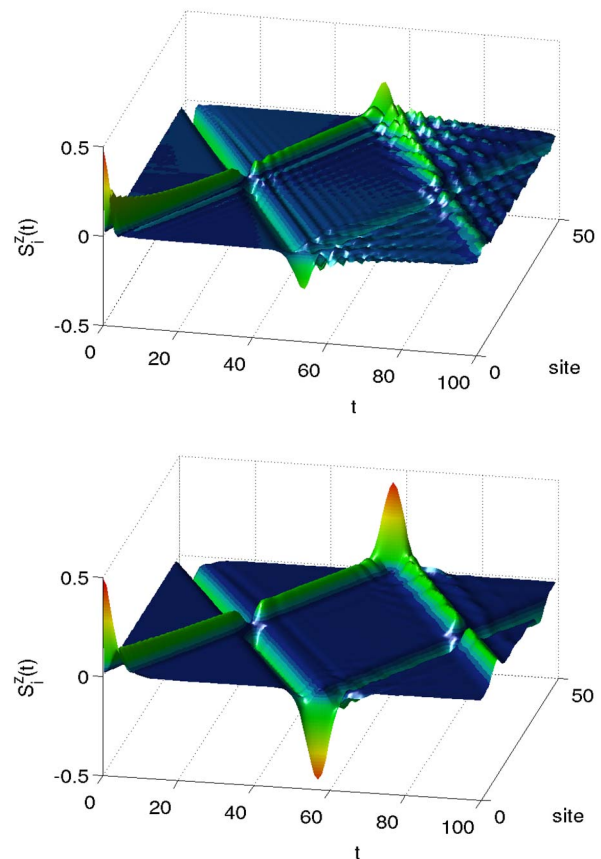


**Figure 3.** Time evolution of the on-site z-magnetization for  $N=50$  and an initial state  $|\uparrow\rangle \otimes |\downarrow\rangle$ ; the qubit-wire coupling is  $j=1$  (top) and  $j=j_{opt}=0.58$  (bottom).

Let us now consider the entanglement transfer in the more general XY model. The dispersion relation is  $\omega_k=[(\cos(k)-h)^2+\gamma^2\sin^2(k)]^{1/2}$ , which is gapped and in particular  $\omega_{k_0} \neq 0$ . Hence, at variance with the XX case, we have to switch on a local magnetic field  $h_0 \sim \omega_{k_0}$  in order to increase the average energy of the initial state and make  $n(k)$  peaked around the linear zone.

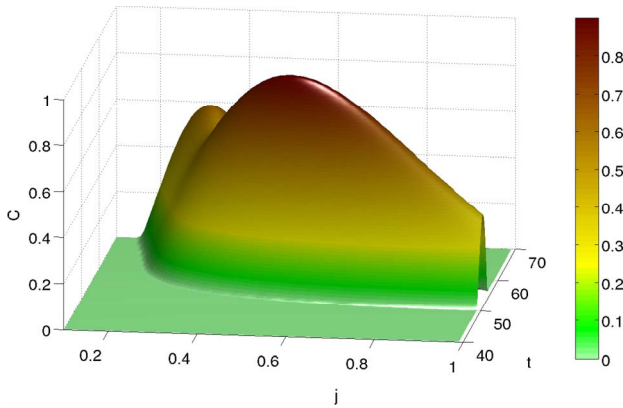


**Figure 4.** Time evolution of the concurrence at varying values of  $j$  for  $\gamma=0$  (XX model) and  $h=0$ . The chain length is  $N=50$ .

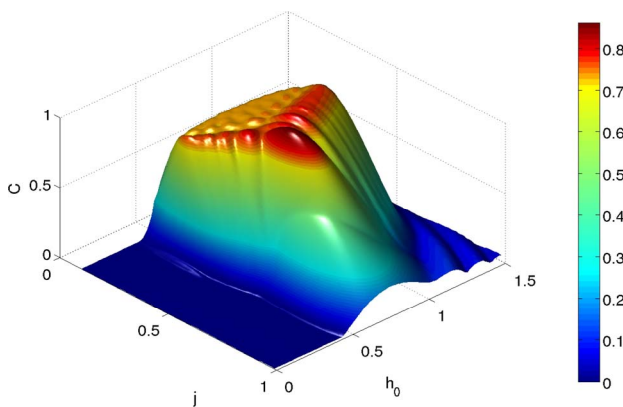


**Figure 5.** Concurrence vs  $j$  and  $h_0$  for  $\gamma = 0.5$  and  $h = 0.54$ . The chain length is  $N = 50$ .

In Fig.5 we plot  $C(t^*)$  for different  $j$  and  $h_0$ , in the XY model with  $\gamma=0.5$  and  $h=0.54$ . It is clear that for fixed  $j$  the best transmission is achieved when  $h_0 \sim \omega_{k0} \sim 0.89$ . With decreasing  $j$ , the distribution  $n(k)$  shrinks in width and the range of the optimal  $h_0$  extends over the whole linear dispersion zone. On the other hand, decreasing  $j$  causes the packet to become delocalized along the chain and the result is that there exists an optimal intermediate value,  $j=0.49$ , in agreement with Eq.(2), for obtaining an almost dispersionless transmission. The region of linear dispersion shrinks for increasing anisotropy  $\gamma$ , while in the Ising limit ( $\gamma=1$ ) with  $h=0$  one has  $\omega_k=1$ , which does not allow for propagation. This explains the observation [18] that in such limit no entanglement propagation takes place: indeed, a vanishing group velocity means that nothing can be transmitted over the chain. However, applying a finite  $h$  on  $\Gamma$  fixes the problem by inducing a finite group velocity. Therefore, one can act on the field so as to fulfil the conditions for optimal dynamics.

In Fig.6 we analyze the entanglement transmission in an Ising chain for various  $h$ , with the optimal value for the parameters  $j$  and  $h_0$ . Raising  $h$  the linear zone gets larger in energy, and, furthermore, the group velocity increases, making the transmission faster and better.

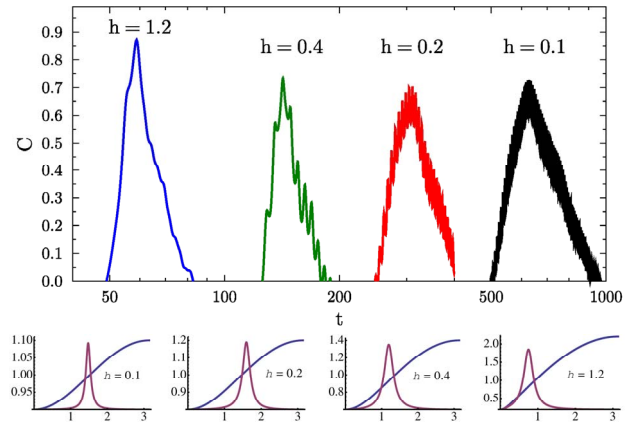


**Figure 6.** Concurrence (top), dispersion relation and density of excitations (bottom) for the case of the Ising chain ( $\gamma=1$ ) for different fields  $h=0.1, 0.2, 0.4, 1.2$ . The corresponding optimized endpoint interactions are  $h_0=0.94, 0.93, 0.82, 0.82$  and  $j=0.39, 0.43, 0.48, 0.48$ . The chain length is  $N = 50$ .

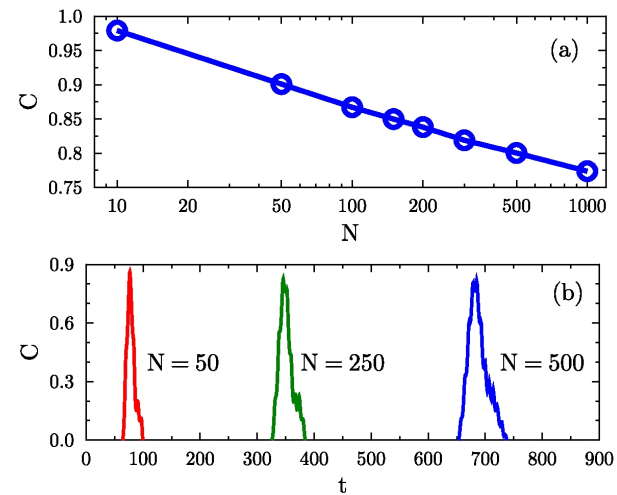


**Figure 7.** (a) Scaling of transmitted concurrence in the XX chain case vs the wire length  $N$ . (b) Time evolution of the concurrence for different channel lengths;  $\gamma=0.5, h=0.54, h_0=0.85$ , and  $j=0.49, 0.39, 0.34$  for  $N=50, 250, 500$ , respectively.

In the XX case, the analytical expression (3) for the optimal coupling allows us to explore the transmission for longer chains. Remarkably, in our scheme the entanglement after transmission is very high also for  $N$  as large as 1000, as shown in Fig.7(a). Despite the XY case being complicated by the need of simultaneously tuning two parameters, very good transmission is obtained also for considerably large  $N$ , as shown in Fig.7(b).

#### 4. Conclusions

We have devised a procedure for achieving high quality entanglement transmission between distant qubits. The procedure relies on tuning the qubit interaction and the coupling with a homogeneous quantum wire in order to induce a coherent ballistic dynamics. There is no need for a specific design neither of the wire, nor of its initial state.

Our approach is then tested with the spin-1/2 XY model and extremely good entanglement transfer is obtained. Due to the induced ballistic dynamics, the transfer time scale is considerably shorter than in previous works [6, 13, 19–21] and essentially depends only on the group velocity of the elementary excitations, which can be increased by varying the parameters of the wire. Moreover, the quality of the state and entanglement transfer that we obtain only weakly deteriorates as the length of the wire increases. Indeed, it is worth noticing that  $\sigma(t) \sim 3/2\sigma$ , i.e., the final optimal packet is just about 22% wider than at start [16], irrespectively of the chain length.

## 5. Acknowledgements

We acknowledge the financial support of the Italian Ministry of University in the framework of the 2008 PRIN program (contract N. 2008PARRTS003). PV gratefully thanks Dr. N. Gidopoulos for useful discussions, and the ISIS Centre of the Science and Technology Facilities Council (UK) for the kind hospitality. PV also acknowledges financial support from the Italian CNR under the “Short-term mobility 2010” funding scheme.

## 6. References

- [1] D. Bruß and G. Leuchs, *Lectures on Quantum Information* (Wiley-VCH, New York, 2007).
- [2] A. Romito, R. Fazio, and C. Bruder, *Phys. Rev. B* 71, 100501 (2005).
- [3] Y. Liu, Y. Zheng, W. Gong, W. Gao, and T. Lu, *Phys. Lett. A* 365, 495 (2007).
- [4] F. de Pasquale, G. L. Giorgi, and S. Paganelli, *Phys. Rev. A* 71, 042304 (2005).
- [5] S. Paganelli, G. L. Giorgi, and F. de Pasquale, *Fortsch. Physik* 57, 1094 (2009).
- [6] S. Bose, *Contemp. Phys.* 48, 13 (2007).
- [7] S. Bose, *Phys. Rev. Lett.* 91, 207901 (2003).
- [8] M. Christandl et al., *Phys. Rev. A* 71, 032312 (2005).
- [9] C. Di Franco, M. Paternostro, and M. S. Kim, *Phys. Rev. Lett.* 101, 230502 (2008).
- [10] T. J. Osborne and N. Linden, *Phys. Rev. A* 69, 052315 (2004).
- [11] H. L. Haselgrove, *Phys. Rev. A* 72, 062326 (2005).
- [12] E. H. Lieb, T. Schulz and D. Mattis, *Ann. Phys.* 16, 407 (1961).
- [13] A. Wójcik, T. Luczak, P. Kurzynski, A. Grudka, T. Gdala, and M. Bednarska, *Phys. Rev. A* 72, 034303 (2005).
- [14] L. Campos Venuti, C. Degli Esposti Boschi, and M. Roncaglia, *Phys. Rev. Lett.* 99, 060401 (2007).
- [15] M. Miyagi and S. Nishida, *Appl. Optics* 18, 678 (1979); *ibid.* 18, 2237 (1979).
- [16] L. Banchi, T. J. G. Apollaro, A. Cuccoli, R. Vaia, P. Verrucchi, *Phys. Rev. A* 82, 052321, (2010).
- [17] W. K. Wootters, *Phys. Rev. Lett.* 80, 2245 (1998).
- [18] A. Bayat and S. Bose, *Phys. Rev. A* 81, 012304 (2010).
- [19] F. Plastina and T. J. G. Apollaro, *Phys. Rev. Lett.* 99, 177210 (2007).
- [20] G. Gualdi, V. Kostak, I. Marzoli, and P. Tombesi, *Phys. Rev. A* 78, 022325 (2008).
- [21] S. I. Doronin and A. I. Zenchuk, *Phys. Rev. A* 81, 022321 (2010).